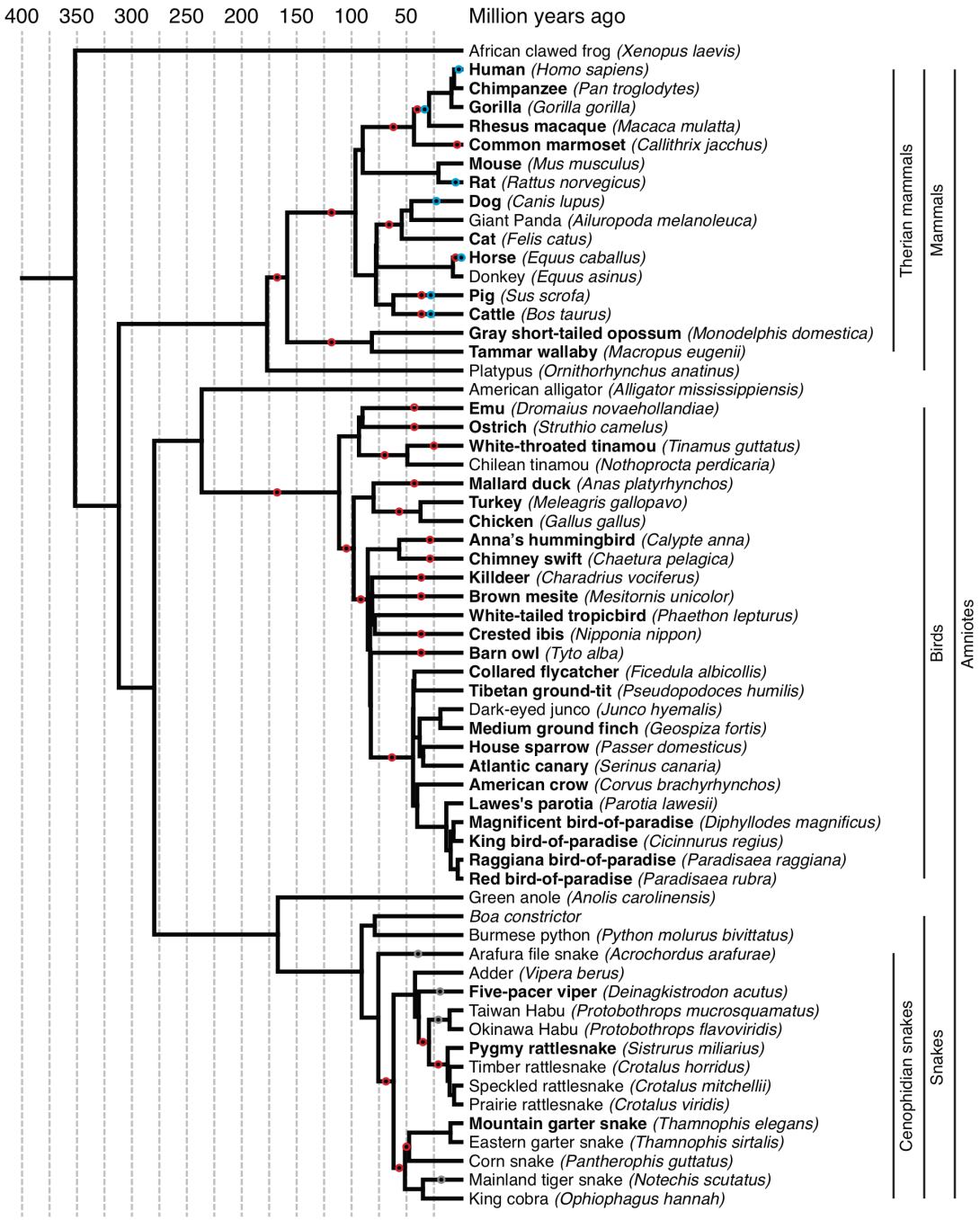

Supplemental Figure S1

Supplemental Figure S1. Phylogenetic tree of selected amniote species.

Phylogenetic tree of amniote species used in this study from TimeTree (Kumar et al. 2017). Species with systematic gene predictions from sex-specific W or Y chromosomes in bold. Red circles mark branches with evolutionary strata with defined boundaries. Blue circles mark branches with X-to-Y transposition events that restored lost ancestral genes to the Y chromosome. Grey circles mark branches with evolutionary strata inferred from phylogenetic analyses of Z–W pairs in snakes, with unknown boundaries. See also Supplemental Tables S8-10.

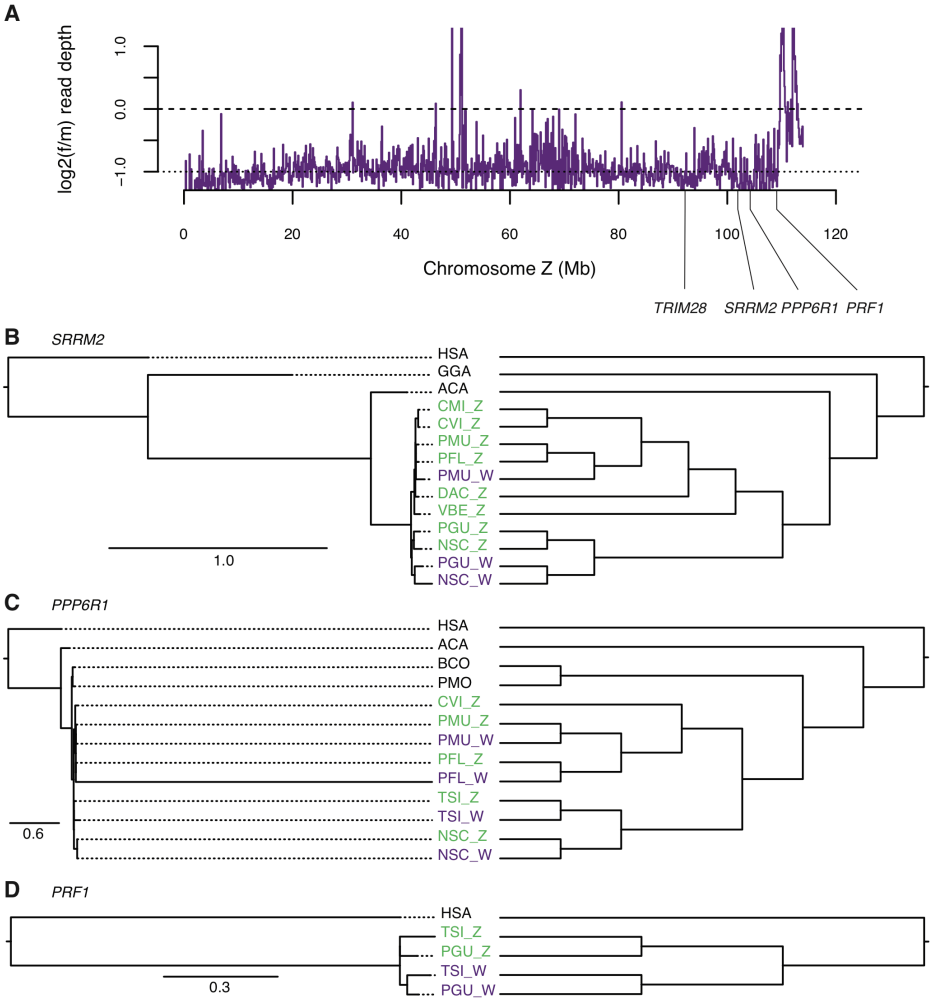

Supplemental Figure S2

Supplemental Figure S2. Lineage specific strata in mountain garter snake.

(*A*) Log2 normalized female/male coverage ratio of mountain garter snake mapped to the prairie rattlesnake reference genome in 100kb windows. The dashed line at

zero represents expectation for diploid sequence; the dotted line at -1 represents the expectation of hemizygous sequence. Best supported gene trees from maximum likelihood and parsimony analysis of (*B*) *SRRM2*, (*C*) *PPP6R1*, and (*D*) *PRF1*. Purple, W-linked homologs; green Z-linked homologs; black, autosomal homologs. Left, maximum likelihood tree; scale bars represent expected number of nucleotide substitutions per site along each branch. Right, cladograms to show topology of short branches. Species abreviations: HSA, human; GGA, chicken; ACA, lizard; BCO, *Boa constrictor*; PMO, python; AAR, Arafura file snake; CMI, speckled rattlesnake; CVI, prairie rattlesnake; CHO, timber rattlesnake; SMI, pygmy rattlesnake; PFL, Okinawa habu; PMU, Taiwan habu; DAC, five-pacer viper; VBE, adder; TEL, mountain garter snake; TSI, eastern garter snake; PGU, corn snake; NSC, mainland tiger snake; OHA, king cobra.

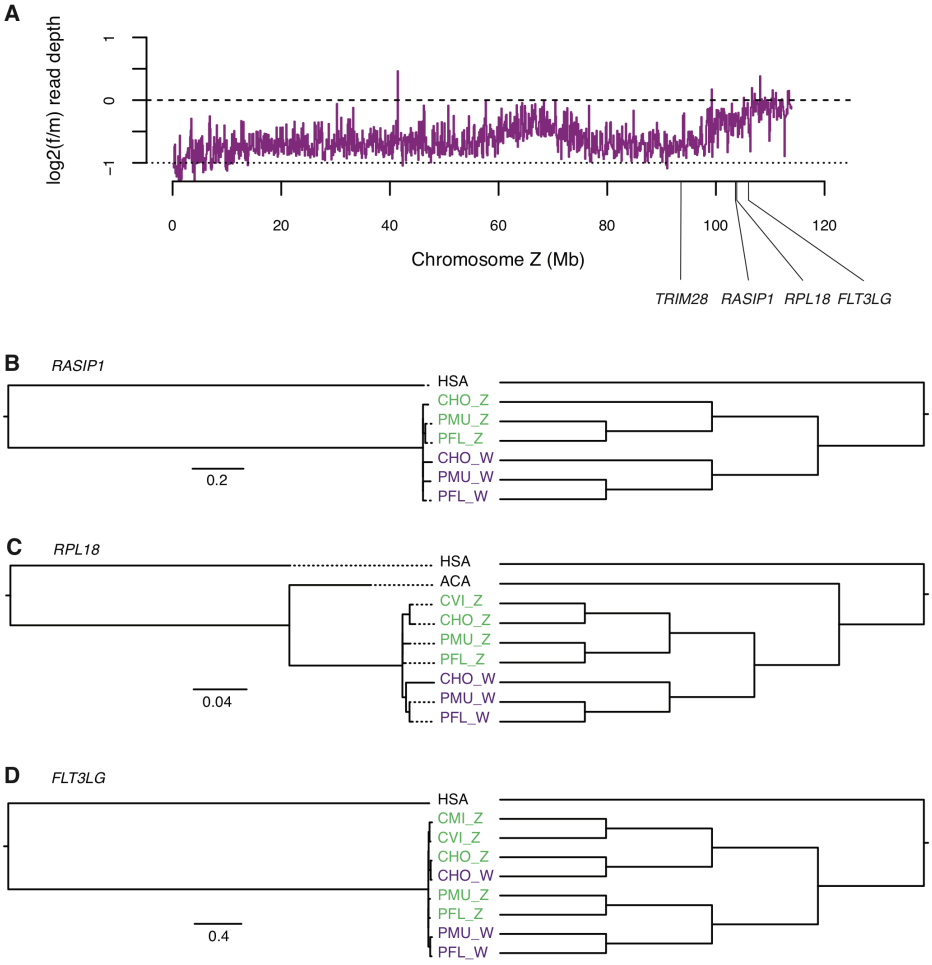

Supplemental Figure S3

Supplemental Figure S3, Lineage specific strata in pygmy rattlesnake.

(*A*) Log2 normalized female/male coverage ratio of pygmy rattlesnake mapped to the prairie rattlesnake reference genome in 100kb windows. The dashed line at zero represents expectation for diploid sequence; the dotted line at -1 represents the expectation of hemizygous sequence. Best supported gene trees from maximum likelihood and parsimony analysis of (*B*) *RASIP1*, (*C*) *RPL18*, and (*D*) *FLT3LG*. Purple, W-linked homologs; green Z-linked homologs; black, autosomal homologs. Left, maximum likelihood tree; scale bars represent expected number of nucleotide substitutions per site along each branch. Right, cladograms to show topology of short branches. Species abreviations: HSA, human; GGA, chicken; ACA, lizard; BCO, *Boa constrictor*; PMO, python; AAR, Arafura file snake; CMI, speckled rattlesnake; CVI, prairie rattlesnake; CHO, timber rattlesnake; SMI, pygmy rattlesnake; PFL, Okinawa habu; PMU, Taiwan habu; DAC, five-pacer viper; VBE, adder; TEL, mountain garter snake; TSI, eastern garter snake; PGU, corn snake; NSC, mainland tiger snake; OHA, king cobra.

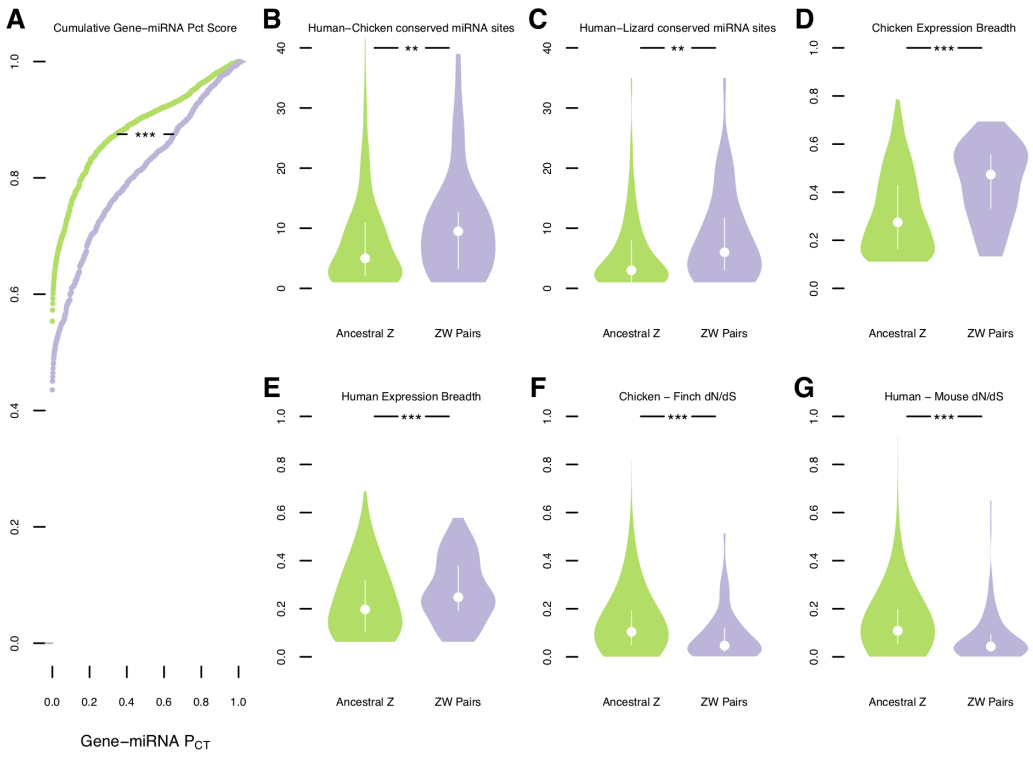

Supplemental Figure S4

Supplemental Figure S4. Additional factors in the survival of caenophidian Z–W gene pairs.

(**) P < 0.01, (***) P < 0.001. Cumulative distribution plot, showing human orthologs of ancestral caenophidian Z–W gene pairs have greater (*A*) PCT scores across all gene–miRNA interactions involving human orthologs of ancestral Z–W gene pairs (purple) than the remainder of ancestral Z genes (green) (two-sided Kolmogorov–Smirnov test). Violin plots, with the median (white circle) and interquartile range (white bar) indicated, compare annotations of ancestral Z–W gene pairs identified in 3 species (purple) to annotations for the remainder of ancestral Z genes (green). P values obtained using one-tailed Mann–Whitney U tests. See Methods and Supplemental Table 5. Human orthologs of ancestral Z–W gene pairs have more miRNA sites conserved between 3′ UTRs of (*B*) human and chicken orthologs and (*C*) human and lizard orthologs than do other ancestral Z genes. Orthologs of ancestral Z–W gene pairs are more broadly expressed than orthologs of other ancestral Z genes (*D*) in a panel of eight adult chicken tissues, and (*E*) in a panel of eight adult human tissues. Orthologs of ancestral Z–W gene pairs have reduced dN/dS ratios compared to orthologs of other ancestral Z genes in

alignments between (*F*) chicken and zebra finch orthologs, and (*G*) human and mouse orthologs.

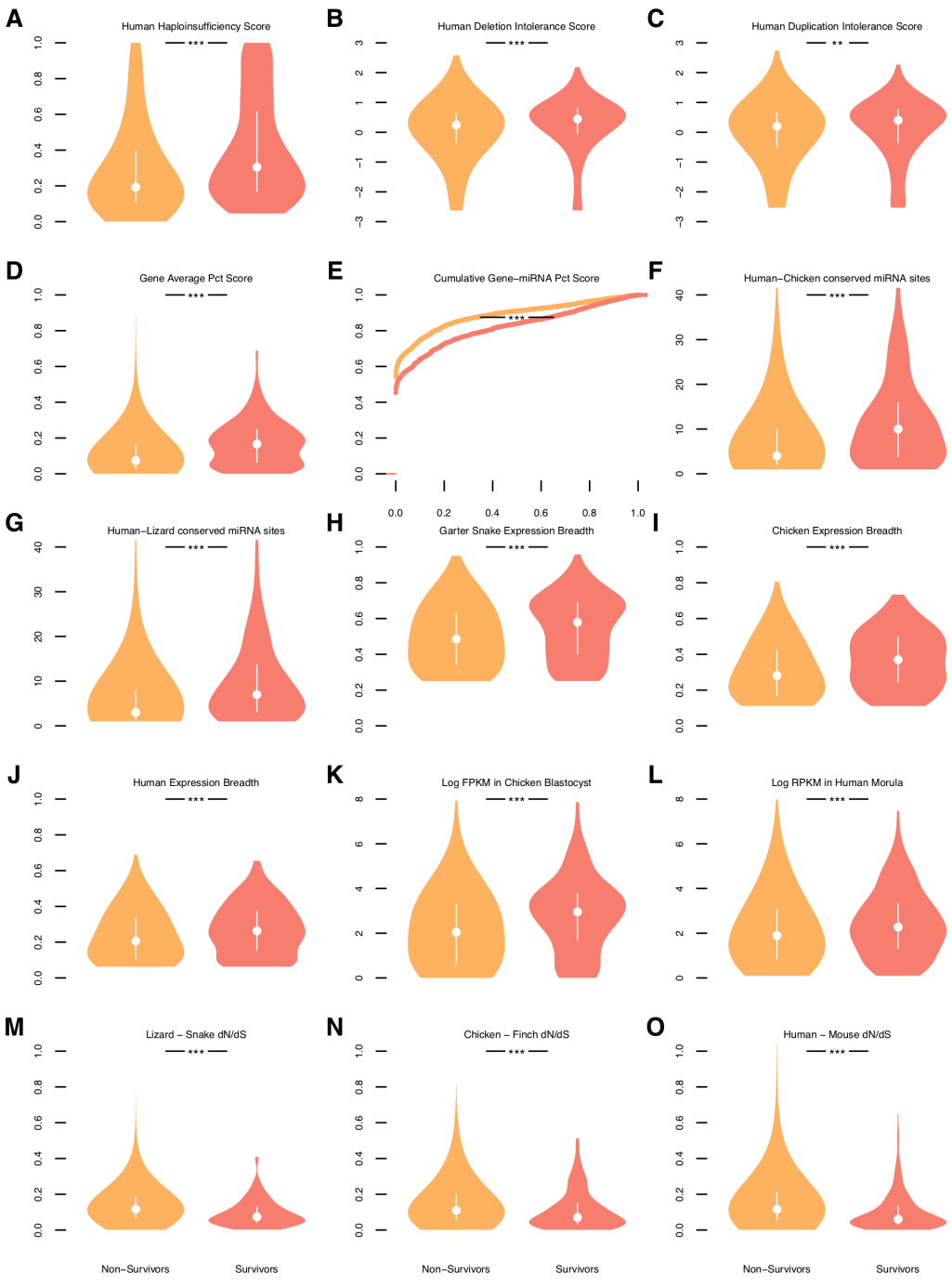

Supplemental Figure S5

Supplemental Figure S5. Factors in the survival of amniote X–Y and Z–W gene pairs.

Violin plots, with the median (white circle) and interquartile range (white bar) indicated, compare annotations of surviving ancestral X–Y and Z–W gene pairs identified in 41 amniote species (red) to annotations for the remainder of ancestral X or Z genes (orange). (**) $P < 0.01$, (***) $P < 0.001$. Unless otherwise noted, P values were obtained using one-tailed Mann–Whitney U tests. See Methods and Supplemental Table 5. Human orthologs of survivors have greater (*A*) probability of haploinsufficiency, (*B*) deletion intolerance scores, (*C*) duplication intolerance scores, and (*D*) mean probabilities of conserved targeting (PCT) than non-survivors. (*E*) PCT score distributions of all gene–miRNA interactions involving human orthologs of survivors (red) and non-survivors (orange) (two-sided Kolmogorov–Smirnov test). Human orthologs of survivors have more miRNA sites conserved between 3′ UTRs of (*F*) human and chicken orthologs, and (*G*) human and lizard orthologs than do other ancestral Z genes. Orthologs of survivors are more broadly expressed than the orthologs of non-survivors (*H*) in a panel of seven adult eastern garter snake tissues, (*I*) in a panel of eight adult chicken tissues, and (*J*) in a panel of eight adult human tissues. Orthologs of survivors are more highly expressed than the orthologs of non-survivors (*K*) in chicken blastocysts, and (*L*) in human preimplantaion embryos. Orthologs of survivors have reduced dN/dS ratios compared to orthologs of non-survivors in alignments between (*M*) tiger snake and green anole lizard orthologs, (*N*) chicken and zebra finch orthologs, and (*O*) human and mouse orthologs.

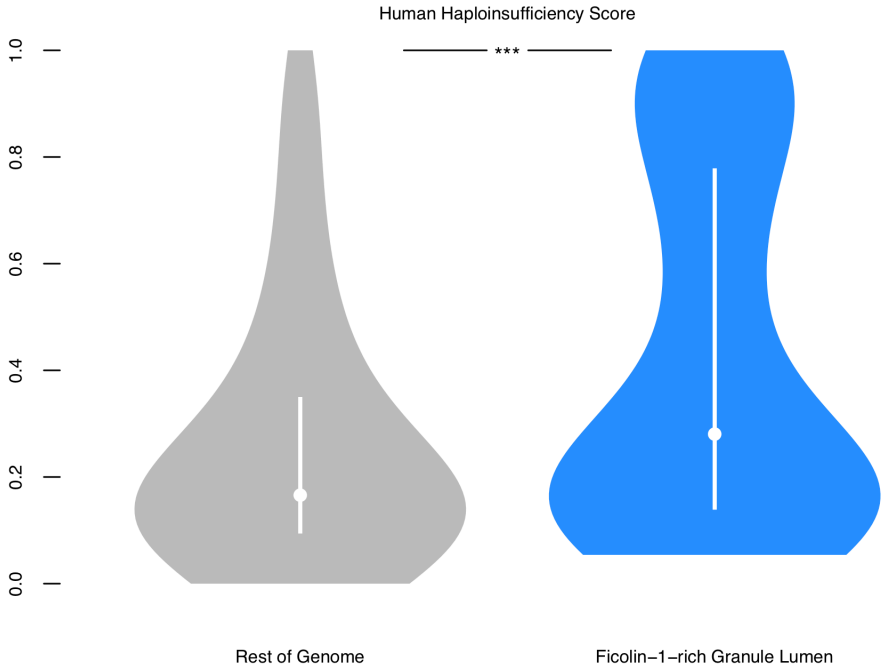

Supplemental Figure S6

Supplemental Figure S6. Components of ficolin-1-rich granule lumen are dosage-sensitive.

Violin plot, with the median (white circle) and interquartile range (white bar) indicated, compares haploinsufficiency of components of ficolin-1-rich granule lumen (blue) to the remainder of genes in the human genome (grey). Components of ficolin-1-rich granule lumen have a greater probability of haploinsufficiency than other human genes (***) $P < 0.001$, one-tailed Mann–Whitney U test.

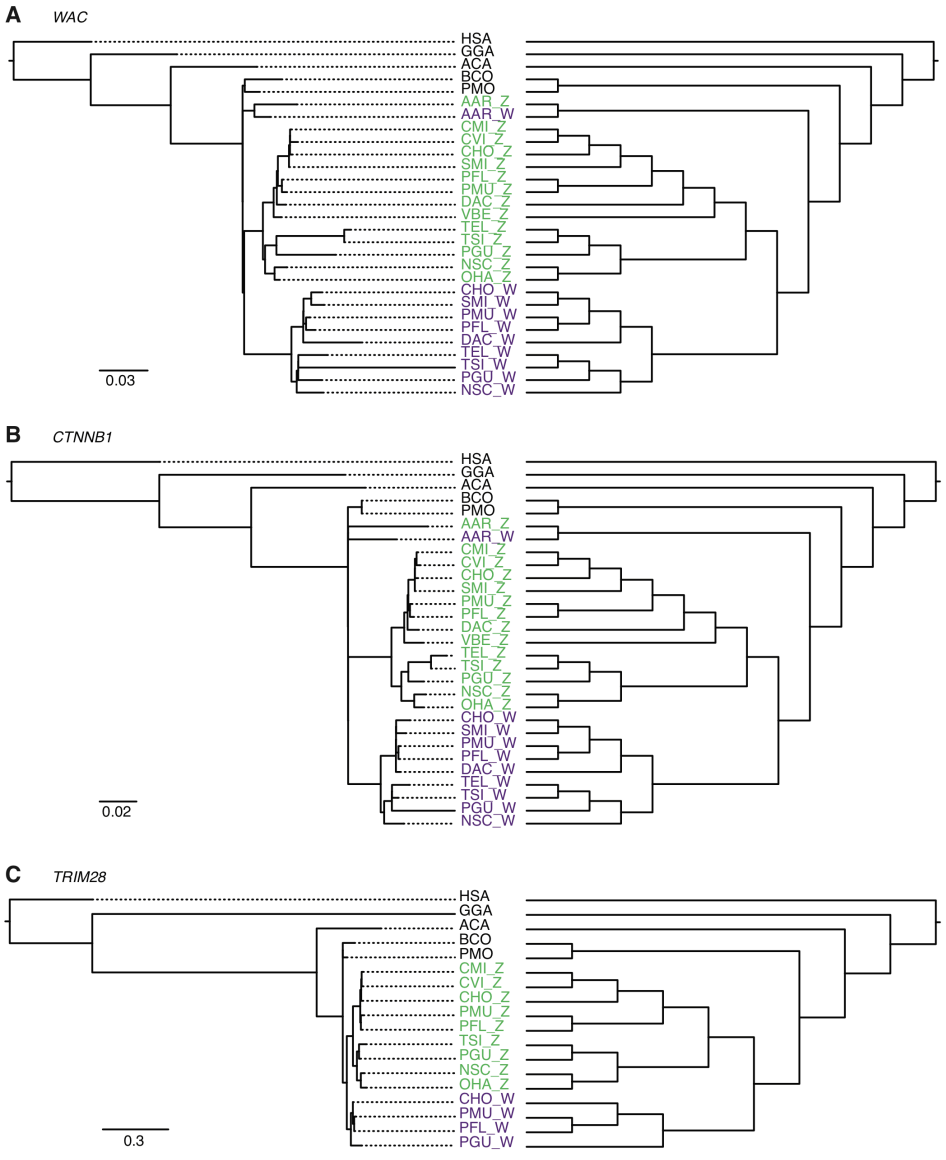

Supplemental Figure S7

Supplemental Figure S7. A large evolutionary stratum formed after vipers and colubroid snakes diverged from Arafura file snake.

Best supported gene trees from maximum likelihood and parsimony analysis of representative genes (*A*) *WAC*, (*B*) *CTNNB1*, and (*C*) *TRIM28*. Purple, W-linked homologs; green Z-linked homologs; black, autosomal homologs. Left, maximum likelihood tree; scale bars represent expected number of nucleotide substitutions per site along each branch. Right, cladograms to show topology of short branches. Species abbreviations: HSA, human; GGA, chicken; ACA, lizard; BCO, *Boa constrictor*; PMO, python; AAR, Arafura file snake; CMI, speckled rattlesnake; CVI, prairie rattlesnake; CHO, timber rattlesnake; SMI, pygmy rattlesnake; PFL, Okinawa habu; PMU, Taiwan habu; DAC, five-pacer viper; VBE, adder; TEL, mountain garter snake; TSI, eastern garter snake; PGU, corn snake; NSC, mainland tiger snake; OHA, king cobra.